

# A Multivalent Hexapod: Conformational Dynamics of Six-Legged Molecules in Self-Assembled Monolayers at a Solid–Liquid Interface

Hong Xu,<sup>†</sup> Andrea Minoia,<sup>‡</sup> Željko Tomović,<sup>§,⊥</sup> Roberto Lazzaroni,<sup>\*,\*</sup> E. W. Meijer,<sup>§,||,\*</sup> Albertus P. H. J. Schenning,<sup>§,\*</sup> and Steven De Feyter<sup>†,\*</sup>

<sup>†</sup>Division of Molecular and Nano Materials, Department of Chemistry, and Institute for Nanoscale Physics and Chemistry, Katholieke Universiteit Leuven, Celestijnenlaan 200 F, B-3001, Leuven, Belgium, <sup>‡</sup>Service de Chimie des Matériaux Nouveaux, Université de Mons-Hainaut, 20, Place du Parc, B-7000 Mons, Belgium, <sup>§</sup>Laboratory of Macromolecular and Organic Chemistry, <sup>||</sup>Institute for Complex Molecular Systems, and Eindhoven University of Technology, P.O. Box 513, 5600 MB Eindhoven, The Netherlands. <sup>⊥</sup> Present address: Elastogran, BASF group, Global PU Specialties Research, GKF/UF, Elastogranstrasse 60, 49448 Lemförde, Germany.

**ABSTRACT** A molecular hexapod having a benzene core and six oligo(*p*-phenylene vinylene) (OPV) legs is an ideal system to probe various types of (intramolecular) dynamics of individual molecules in physisorbed self-assembled monolayers at a solid–liquid interface. Scanning tunneling microscopy reveals that molecules adsorb in 2D crystalline as well as disordered domains. Strikingly, not all molecules have the six OPV units in contact with the graphite substrate: 4% of the molecules in the 2D crystalline domains and up to 80% of the molecules in the disordered domains have one or two OPV units desorbed. In addition, the presence of such a defect promotes the coexistence of another defect adjacent to it. Time-dependent STM experiments and molecular dynamics simulations reveal in detail the different dynamics involved and the multivalent nature of the interactions between hexapod and surface.

**KEYWORDS:** dynamics · monolayer · conformation · translation · scanning tunneling microscopy · self-assembly

Self-assembly of nanometer-sized building blocks into well-defined molecular architectures at surfaces represents one of the important challenges of supramolecular chemistry and material sciences, given the perspective of applications in the broad area of nanotechnology.<sup>1</sup> An increasing popular bottom-up approach for the formation of molecular patterns is self-assembly *via* physisorption at a solid–liquid interface.<sup>2,3</sup> In contrast to, for instance, the well-known class of self-assembled monolayers of alkylthiols chemisorbed on gold,<sup>4</sup> physisorbed alkylated molecules lie most often flat on an atomically flat substrate, such as gold or graphite, and often form two-dimensional (2D) crystalline lattices with a periodicity between 1 and 10 nm. Exploring the dynamics of molecules in such physisorbed self-assembled monolayers is of importance since dynamic processes may determine

the final properties of the system. However, probing these dynamics is very challenging since the molecules are part of a monolayer and often packed in a 2D lattice. Fortunately, scanning tunneling microscopy<sup>5</sup> (STM) makes it possible to image individual molecules with submolecular resolution and to probe their supramolecular interaction modes<sup>6–8</sup> and dynamics.<sup>9,10</sup> Especially ultrahigh vacuum (UHV) conditions combined with temperature control turn out to be ideal to probe the spontaneous dynamic behavior of molecules. Several exciting phenomena were discovered, such as translational,<sup>11–18</sup> rotational,<sup>19–21</sup> and conformational dynamics<sup>22–27</sup> or a combination thereof of single molecules or clusters on atomically flat metallic surfaces. Sometimes these dynamics were intentionally provoked by the interaction with the STM tip.<sup>28–38</sup>

The observation of molecular dynamics at the single-molecule level using STM at solid–liquid interfaces imposes a number of challenges though. Under physisorption conditions, at room temperature, most low molecular weight molecules are too mobile to be visualized, except if they are trapped in a 2D (crystalline) matrix. Any vertical motion (*e.g.*, the desorption of a molecule from the monolayer into the liquid phase and the adsorption of a molecule from the liquid phase into the monolayer at the same site) occurs very fast and goes normally unnoticed, except if marker molecules are used to observe these out-of-plane dynamics.<sup>39,40</sup> Likewise, typically no

\*Address correspondence to roberto@averell.umh.ac.be, e.w.meijer@tue.nl, a.p.h.j.schenning@tue.nl, steven.defeyter@chem.kuleuven.be.

Received for review February 9, 2009 and accepted March 26, 2009.

Published online April 10, 2009.  
10.1021/nn900131k CCC: \$40.75

© 2009 American Chemical Society

spontaneous conformational changes at the single-molecule level are observed in the “bulk” of such molecular monolayers. The few studies on spontaneous dynamics at the solid–liquid interface mainly deal with Ostwald ripening,<sup>41–43</sup> that is, the growth of larger domains at the expense of smaller ones or the conversion of one polymorph (phase) into another polymorph (phase).<sup>44,45</sup> These spontaneous processes involve (collective) changes in molecular orientation (translation/rotation) and possibly also conformation, though the latter events have rarely been probed at the single-molecule level.

A powerful and versatile tool to obtain stable patterned monolayers is the use of multivalency in which a multivalent agent is binding to a surface.<sup>46,47</sup> Due to the so-called effective concentration, leading to high affinity, and the low dissociation rate, thermodynamic and kinetic stable monolayers can be obtained. The understanding and visualization of multivalency is of great importance for the creation of well-defined patterned monolayers. Time-dependent STM seems to be an attractive technique to monitor this phenomenon.

We have used an ultrapure, six-legged oligo(*p*-phenylene vinylene) (OPV)-substituted hexaarylbenzene **1** (Figure 1) that acts as molecular “hexapod” in a self-assembled monolayer at the solid (highly oriented pyrolytic graphite)–liquid (1-phenyloctane) interface. Recently, we have shown that this compound self-assembles in solution into perfect 1D fibers by a nucleation–growth mechanism. The chirality of the 24 stereocenters is expressed at the supramolecular level, indicating the cooperative nature of the packing.<sup>48</sup> Moreover, at the solid–liquid interface, a well-ordered 2D lattice was formed, again with an expression of chirality at the supramolecular level.

In this paper, we reveal a multitude of dynamical events taking place in the monolayer. Due to the multivalent interaction, as result of the six OPV legs, the dynamics of **1** with the substrate is slow on the STM time scale, enabling us to visualize its orientational, conformational, and translational behavior at the single-molecule level at the solid–liquid interface.

## RESULTS AND DISCUSSION

**Conformational Flexibility:** Upon applying a drop of solution containing **1** on top of the basal plane of highly oriented pyrolytic graphite, by self-assembly the spontaneous formation of a monolayer sets in. Large- and small-scale STM images recorded at the interface between graphite and 1-phenyloctane are shown in Figure 2, and the main structural characteristics of the molecules can easily be appreciated. The OPV units appear bright in the STM image, while the orientation of the alkyl chains is hardly visible. Those bright features typically reflect the anticipated star shape of the molecules.<sup>48</sup> Space considerations and the few images where the alkyl chains can be identified point out that

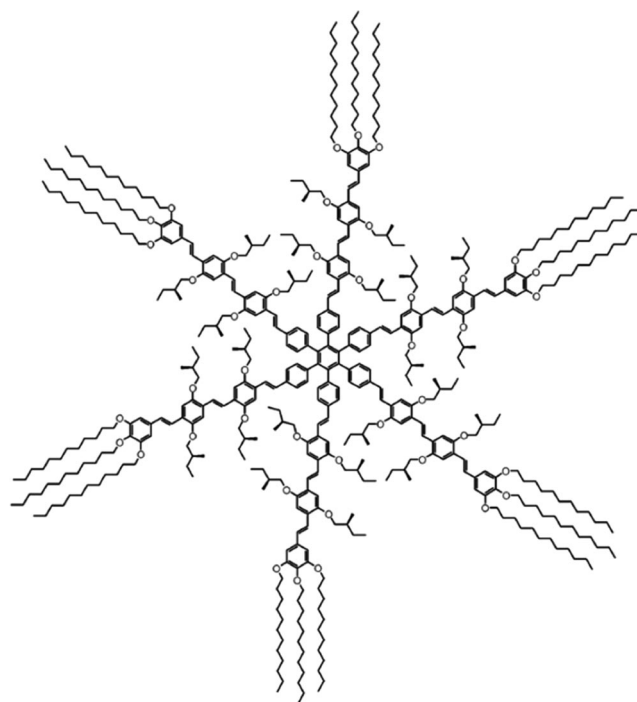


**Figure 1.** Chemical structure of the six-legged oligo(*p*-phenylene vinylene)-substituted hexaarylbenzene **1**.

only two out of three alkyl chains are adsorbed on the surface. These are basically aligned along one of the main symmetry axes of graphite. Also the unit cell vectors are aligned along the main symmetry axes of graphite ( $a = b = 5.56 \pm 0.07$  nm; the angle between both unit cell vectors measures  $61 \pm 2^\circ$ ), although some exceptions have been observed.

Structurally defect-free 2D crystalline domains covering large areas are not observed though. Often “disordered” domains are observed in the midst of or between these crystalline domains. We identify a group of molecules as belonging to a disordered domain if the centers of the molecules are not on top of 2D crystalline lattice points within a given area or if the molecules have a different orientation than those in the crystalline matrix. In total, the appearance of more than 20 000 molecules was evaluated by a human observer. About 2/3 of these molecules self-assemble into a regularly ordered matrix; 1/3 of the molecules are adsorbed in what we define as disordered domains.

Some of these molecules *appear* to have only five or four legs, as illustrated in Figure 2C. Strikingly, the situation in the so-called ordered and disordered domains is completely different. In ordered areas, most of the molecules appear as six-legged molecules (96.0%); 3.3% of the molecules appear with five legs and only 0.7% with four legs. In contrast, this ratio differs drastically in disordered domains. First note that a significant fraction (almost 1/3) of the molecules in the so-called disordered domains are badly resolved, and it is not possible to identify their appearance (six or five or four legs) with certainty. However, of the remaining 3803

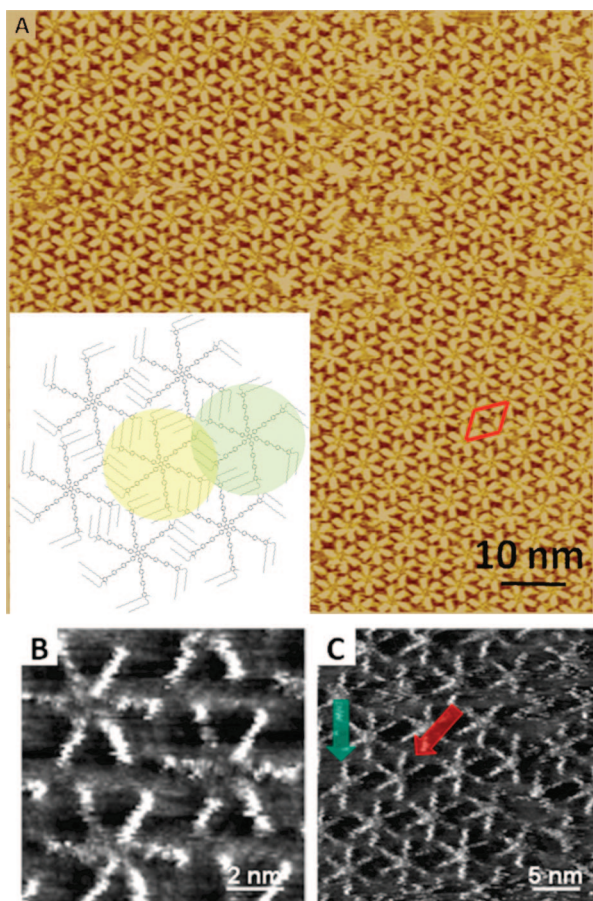


**Figure 2.** STM images of monolayers of **1** physisorbed at the solid (graphite)–liquid (1-phenyloctane) interface;  $I_{\text{set}} = 0.60$  nA,  $V_{\text{set}} = -0.31$  V. (A) Large domain,  $I_{\text{set}} = 0.05$  nA,  $V_{\text{set}} = 0.8$  V. Inset: Model reflecting the ordering of the molecules in a 2D crystal. Two alkyl chains per OPV leg are adsorbed. The third one, which is omitted in the model, is most likely solvated. For clarity, the chiral 2-methylbutoxy groups are not shown. The intersection of the two colored disks coincides with the area of interaction between these two adjacent hexapods. A unit cell is indicated in red. (B) Magnified image showing the expected star shape of the molecules. (C) In addition to the six-legged molecules, molecules are visible with apparently only five (red arrow) or even four legs (green arrow).

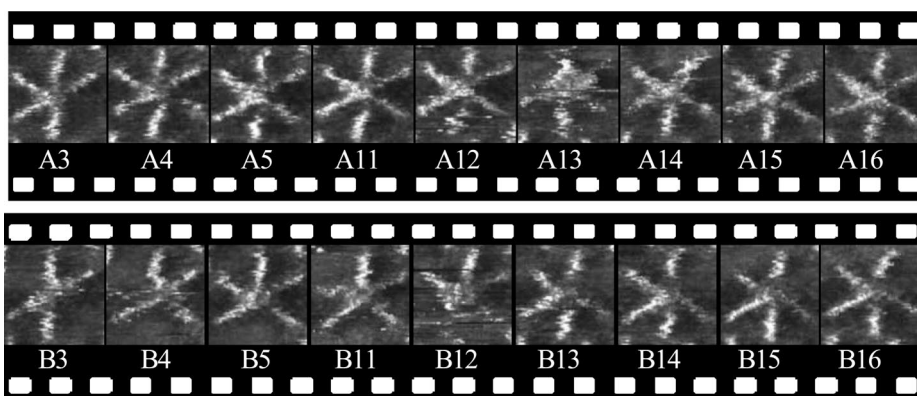


**Figure 3.** Sequence of STM images zooming in on one molecule. Top: molecule A. Bottom: molecule B. The frame numbers are indicated below each image. The time difference between two consecutive frames (e.g.,  $A_n \rightarrow A(n + 1)$ ) is about 14 s.

molecules, only 23% appear as six-legged molecules, while the majority of the molecules (57%) appear with five legs and 20% of the molecules in disordered domains show four legs.

This detailed analysis led to some more remarkable results when we investigated the distribution of these defects (so the molecules which appear with five or four legs) in the 2D crystalline areas. On the basis of the fact that the 2D crystalline hexagonal lattice contains 4.0% of defects, it is predicted that about 27% of these defects would appear in dimers. In contrast, experimentally, a significantly higher population of molecules in dimers is observed (40%), indicating that a defect promotes the presence of another one in its periphery (see Supporting Information).

In addition to the fact that synthesis and purification were carried out according to the highest possible standards making use of recycling GPC,<sup>48</sup> the appearance of the molecules changed during the STM acquisition, that is, as far as the number of visible legs and their orientation is concerned. This was interpreted as definite proof that the “defective” molecules are not impurities (*vide infra*).

**Conformational Dynamics:** Certain molecules show indeed some interesting changes in appearance. Quite often, the number of “legs” changes; legs disappear and reappear. Figure 3A shows a series of images zooming in on the different appearances of one molecule as a function of time (molecule A).

In frame A3, the molecule only shows five legs; the leg at 4 o’clock is missing, while in frame A4, all legs are visible. The image in frame A13 is blurred and marks the transition from six visible legs (frame A12) to five visible legs (frame A14). In frame A15, all six legs appear again. Another example of a similar transition is shown in Figure 3 (bottom). This molecule starts off with four visible legs (frame B3) and evolves into a situation where five legs are visible (from frame B5 on).

Not only does the *number* of visible legs change but their *orientation* changes in time. Basically, two types

of orientational changes can be observed. A first type involves a transition where the desorption–adsorption of legs results in an apparent rotation of the molecules. For instance, in Figure 4A, at the position of the red arrow, a leg appears, while at the position of the green arrow, a leg disappears. Overall, the molecule appears to be rotated. This rotation hypothesis is unlikely as it involves the desorption and adsorption of all legs. Note that the position of the other legs has not changed.



In addition, these molecules are not rigid as far as the position of the legs is concerned. The molecule in Figure 4B undergoes a transition from five adsorbed legs to six adsorbed legs. Note, however, that the “readsorption” of the sixth leg follows the reorientation of the leg indicated in green: originally at 1 o’clock, it appears subsequently at the 12 o’clock position. Also more subtle orientational changes can be observed (Figure 4C). The legs indicated by the red arrows slightly change their orientation from frame to frame, though the overall orientation of the molecule remains unchanged. The effect is that the angle between the legs is not always 60° but can change considerably.

These data strongly suggest that the origin of the “defects” is the desorption/readsorption or reorientation of legs. More evidence will follow for the fact that the disappearance and reappearance of the bright legs are not merely due to differences in the tunneling efficiency as the result of orientational changes that do not involve desorption of the legs.

With the disappearance and reappearance events of the legs being identified as the desorption and readsorption of these legs, respectively, one can now estimate the differences in energy between a six-legged molecule and molecules with five or four adsorbed legs in 2D crystalline lattices based on a Boltzmann distribution: this value is 0.097 eV for a molecule with one leg desorbed and 0.14 eV for a molecule with two legs desorbed (see Supporting Information). These values are much lower than one could expect based on the adsorption energy of an alkyl chain on graphite, which is about 0.07 eV/CH<sub>2</sub>.<sup>18</sup> Therefore, solvation of the OPV unit and alkyl chains must be crucial to support the desorption process of individual legs.

In addition, the larger than statistically predicted number of dimer defects in the 2D crystalline lattice indicates that molecules mutually interact and that desorption of a leg in a hexapod promotes the desorption of a leg in a hexapod next to it. Some clue to the origin of this behavior comes from a detailed analysis of the nature of these dimers. Basically, we have evaluated the relative orientation of the desorbing OPV units in dimers where both molecules have five OPV units adsorbed. Of the 21 possible combinations, one is, in particular, favored: it is the combination where both parallel OPV units of which the alkyl chains in principle could interact *via* van der Waals interactions (see also intersection of disks in insert of Figure 2A) are desorbed (11 dimers or 17%). Its occurrence is much more frequent than what is to be expected on statistical grounds (2.78%; see Supporting Information). The desorption of a leg has therefore a direct impact on the stability of the OPV leg in the adjacent hexapod it is interacting with and favors its desorption.

An attempt was made to investigate some aspects of the conformational dynamics by molecular modeling.

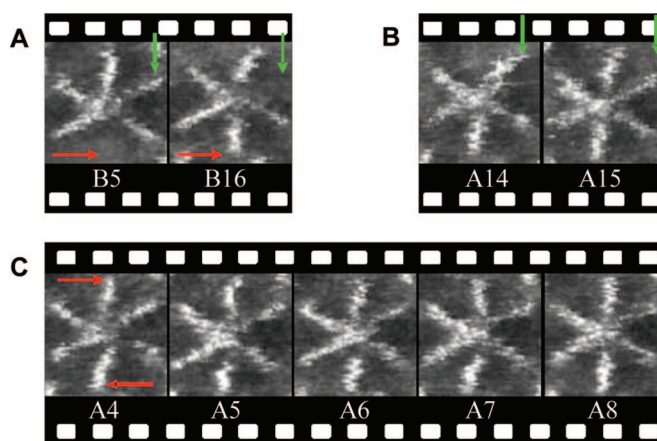


**Figure 4.** Sequence of STM images zooming in on one molecule highlighting different dynamics. (A) The molecule *appears* to rotate. At the position of the red arrow, a leg appears, while at the position of the green arrow, a leg disappears. (B) Readsorption of a leg, affecting the orientation of the leg originally at 1 o’clock. (C) The legs indicated by the red arrows slightly change their orientation from frame to frame, though the overall orientation of the molecule remains unchanged. The frame numbers are indicated below each image. The time difference between two consecutive frames is about 14 s.

lular modeling package TINKER 4.2<sup>49</sup> using the MM3(2000) force field.<sup>50</sup> This force field has been recently parametrized to give an accurate description of weak intermolecular interactions, which are likely to play an important role in physisorption and self-assembly phenomena. For computational reasons, two simplifications were made: (1) the modeling involved only one molecule adsorbed on graphite, and (2) the dodecyloxy groups were replaced by ethoxy groups. These simulations are therefore not intended to reproduce the experimental data but to shine light on the intrinsic conformational properties of the conjugated moieties of the molecule, so ignoring the effect of alkyl chain–graphite interactions and alkyl chain–alkyl chain interactions between adjacent molecules. The main conclusions are the following (for a detailed description, see Supporting Information).

In a first simulation, the readsorption process was followed by molecular dynamics in the presence of solvent. For that purpose, we modeled a molecule having already one leg pointing in the solvent phase and let the molecule relax. As expected, molecular dynamics showed that the phenyl rings attached to the central benzene ring are rotated to form a kind of chiral propeller and make the adsorption of the central benzene to the graphite difficult. The atoms of the next phenyl groups are not significantly out of the plane of the molecule at the surface, while the largest variations occur for the atoms close to the extremity of the leg. Interestingly, at the end of the simulation, the leg is fully adsorbed on the surface, which means that one leg can desorb and be readsorbed despite the lateral relaxation of the other legs (*i.e.*, the fact that parts of the neighboring legs may slide and fill the space left empty by the desorbed leg). The terminal phenyl ring can adsorb flat,

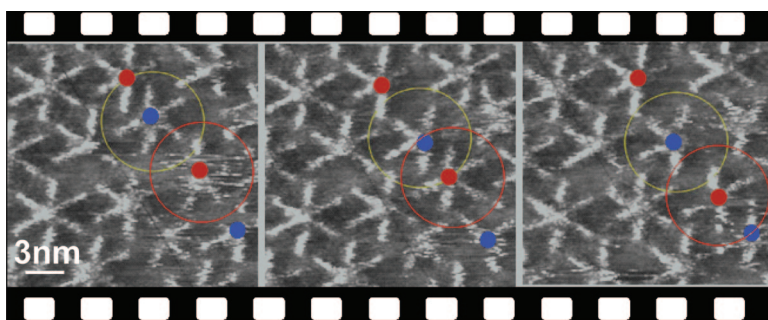


**Figure 5.** Sequence of STM images zooming in on conformational and translational events of **1** at the solid–liquid interface. The time gap between the frames is 26 and 68 s. Colored disks and circles indicate the center and periphery of a number of selected molecules, respectively.

with strong  $\pi$ – $\pi$  interactions with graphite, while the tilting of the phenylene units closest to the core (due to steric hindrance) induces the core ring to be slightly “lifted up” with respect to the equilibrium adsorption distance for an unperturbed benzene ring.

In a second set of simulations, the lateral mobility was modeled for the legs remaining adsorbed on graphite (*cf.* frames B14–B16 in Figure 3) when one leg is desorbed. For practical reasons, a molecule on the surface having *in silico* one leg chopped off was considered, with only the first phenyl ring left since this is the part of the leg that cannot desorb. We followed the lateral mobility of the adsorbed legs (i) in terms of the angle between opposite legs with respect to the center of the molecule and (ii) in terms of the distance between the ends of the legs adjacent to the desorbed one. The results show relaxation of the molecule expressed by a displacement of the two adjacent adsorbed legs toward the empty space resulting from the missing leg combined with a breathing motion of those legs, while the behavior of the three other legs is not affected (see Supporting Information).

**Translational Dynamics:** In the conformational dynamics presented, simulated, and discussed above, the position of the center of mass of the molecules was not found to change. However, in addition, translational motion was also observed, as highlighted in Figure 5. In this sequence of images, there is translational motion on the surface in areas that are characterized by nonideal ordering of the molecules, in other words in areas with free space. For the molecules that are indicated by the colored rings, the center of mass position changes. Those molecules, which undergo translational changes, simultaneously also undergo orientational changes of their legs (see also the movie in Supporting Information). Due to the limited number of observations, no conclusions can be drawn if certain translational directions, for example, along one of the symmetry axes of graphite, are preferred.

Can one be sure that orientational/translational motions take place in the plane of the substrate? Though it is appealing to consider that these molecules are

moving on the surface, there is also the possibility of molecular desorption–adsorption dynamics (*i.e.*, vertical dynamics) as the experiments are carried out at the solid–liquid interface. Desorption–adsorption phenomena have been demonstrated for alkylated isophthalic acid derivatives and other alkylated molecules.<sup>39,40</sup> However, for the hexapod system, the desorption–adsorption dynamics are considered to take place at a much longer time scale than observed for smaller alkylated systems. One molecule has 18 dodecyloxy chains. Even if only a fraction of the alkyl chains are adsorbed, the overall interaction energy at 0.07 eV/CH<sub>2</sub> is sufficiently high to slow down the desorption dynamics considerably.<sup>18</sup> Therefore, it is safe to conclude that the observed dynamics are surface-confined and do not reflect desorption–adsorption dynamics.

The translational dynamics confirms also that the disappearance and reappearance of the bright legs is due to a desorption–readsorption process and not to a change in electron tunneling efficiency through the OPV legs as a result of some other orientational changes. Consider, for instance, the two molecules marked in the upper half of the left frame of Figure 5. In both molecules, only five legs are visible. The invisible legs must be desorbed from the surface: the core to core distance between these “colliding” molecules (3.91 nm) and the distance between parallel legs (1.82 nm) are much smaller than for the regular arrangement, and there is just no space for the “sixth” leg of each molecule to be adsorbed (see Supporting Information). In line with the previous arguments, the apparent rotation of five-legged molecules (Figure 4A) should be described as the desorption of one leg and the simultaneous adsorption of another leg, rather than the rotation of the molecules within the plane of the substrate or a molecular desorption–adsorption process.

Figure 6 shows a comparative histogram of the nearest neighbor distance (measured between the central phenyl groups) in ordered and disordered areas. Clearly, disorder goes along with an on average reduced nearest neighbor distance. The clear bias toward smaller values for disordered domains explains in part the drastic difference in population in ordered and disordered domains. At small intermolecular distances, the molecules cannot have all OPV legs adsorbed because of steric hindrance, as illustrated above, naturally leading to a shift in population from molecules with all OPV units adsorbed to molecules with only five or four OPV units adsorbed.

**Random or Collective Processes?** In the previous paragraphs, we have described different dynamics (desorption–adsorption of legs), orientational/conformational flexibility, and translation at the level of individual molecules. This description did not take into ac-



count the relation between the motion of individual molecules and the (lack of) dynamics of its surroundings. Figure 7 summarizes the different aspects of the motion by a color code revealing the following: (i) desorption–readsorption phenomena of individual legs occur both in a noncorrelated (green) and correlated (yellow) fashion; (ii) a reorientation of the legs (e.g., a five-star that “rotates”) goes always together with the desorption or reorientation of legs of adjacent molecules; (iii) not surprisingly, quite some conformational dynamics occurs in the area of the translationally mobile molecules. The conclusion to draw is that the conformational or translational motion of a given molecule will favor simultaneous dynamics of adjacent molecules. This is in line with the steady-state picture which revealed the high tendency to form dimer defects.

How can we now account for the huge difference in population in ordered and disordered domains? Basically, the data show that both reduced intermolecular interactions and increased intermolecular interactions promote the conformational dynamics.

When being part of a 2D crystalline lattice, the molecules are trapped and stabilized by intramolecular and intermolecular alkyl chain–alkyl chain van der Waals interactions. Only a small percentage of molecules have one or two legs desorbed (4%). The presence of a defect was shown to promote the coexistence of another defect adjacent to it.

When being part of a disordered domain, the majority of the molecules (77%) appear as defects. This is in part due to the molecular mobility and the on average reduced distance and increased intermolecular interactions between molecules (steric hindrance). In addition, reduced alkyl chain–alkyl chain interdigitation interactions most likely contribute to the high fraction of defect sites.

**Multivalency:** Another way to look at the peculiar dynamic behavior of the hexapod is the following. If the total interaction energy with the substrate would be too strong (van der Waals interactions between the six OPV units, the alkyl chains, and the substrate), the mobility of such a molecule would be very slow and it would take a long time before ordered self-assembly sets in. For having such a strong interaction, all six legs should be able to be adsorbed in a perfect way, or in other words, self-assembly would be impaired, or the self-assembly kinetics

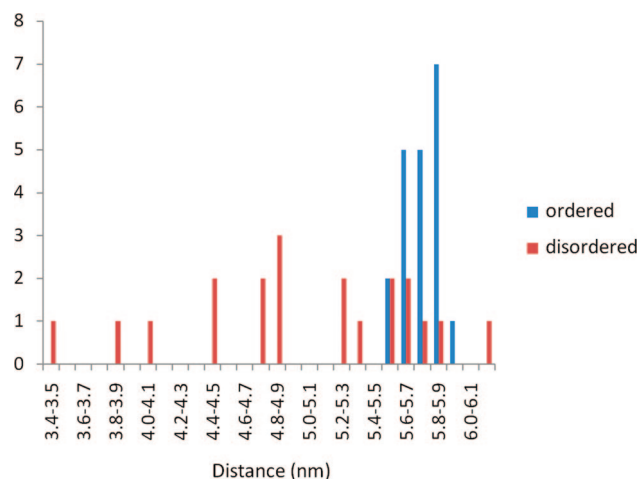


Figure 6. Histogram of the nearest neighbor distance in ordered and disordered domains.

too slow, if the multivalency<sup>51</sup> effect is too strong. When the fit between molecule and surface is just off, this “wrongly” designed multivalency favors the self-assembly process to set in relatively fast. In that case, a limited number (four or five) of legs will be adsorbed

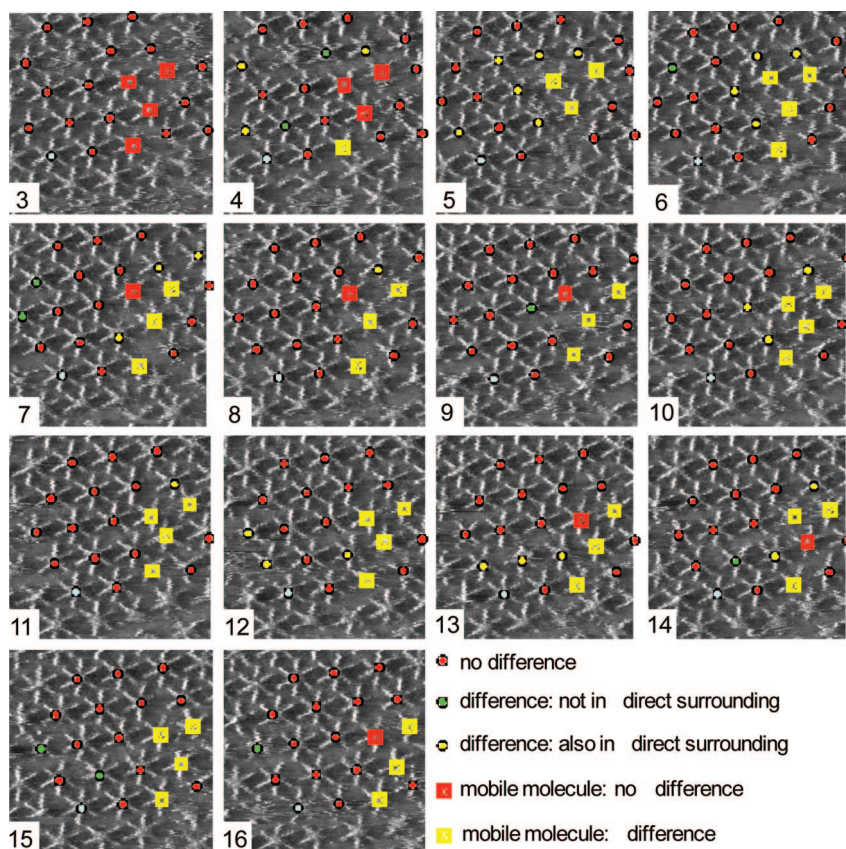


Figure 7. Color-coded sequence of STM images. The center of a molecule is indicated by a disk (translational immobile) or square (translational mobile). Red indicates that there is no difference with the previous frame. Green indicates there is a difference in the number of legs adsorbed or orientation with the previous frame. However, no apparent change is observed in the surrounding molecules which could be correlated with that motion. Yellow indicates there is a difference in the number of legs adsorbed or orientation with respect to the previous frame. Changes are observed in the surrounding molecules too. The blue disk is a reference point. The frame number is indicated in the lower left corner.

perfectly, while the remaining ones are searching for their ideal binding place. On average, the binding of all six legs is diminished compared to a perfectly fitted hexapod molecule.

In conclusion, we have demonstrated and visualized conformational dynamics of individual molecules, resembling molecular hexapods, in a self-assembled monolayer at a solid–liquid interface by STM. The dynamics reflects to some extent the motion of hexapods, occurs “spontaneously”, and is not the result of heat or light treatment nor is it induced by STM tip manipulation. Intramolecular conformational dynamics were shown to be promoted by nearest neighbor interactions. In addition, translational motion of individual molecules was observed, which could be correlated with conformational dynamics that occurred simultaneously.

This high molecular weight molecule allows probing dynamic phenomena at a solid–liquid interface in a unique way. However, conformational and translational dynamics are by no means unique to this molecule. Upon self-assembly into 2D crystalline matrices, the typically low molecular weight molecules probably undergo (slight) conformational dynamics, but these dynamical phenomena are expected to occur so fast that averaged images are obtained: the different con-

formational states are not resolved.<sup>52</sup> Thanks to the specific structure of the molecular hexapod and its size, giving rise to a relatively large interaction with graphite, these submolecular dynamic phenomena could be followed. Molecular dynamics simulations confirmed the possibility of adsorption/desorption processes for individual legs.

Out-of-plane conformational dynamics also relate to the vertical dynamics—adsorption and readsorption—of small molecular weight molecules at a solid–liquid interface, mediated by desolvation and solvation. In physisorbed systems at a solid–liquid interface, these desorption–adsorption dynamics typically remain unnoticed—the site of a desorbed molecule is immediately filled by another one—except if marker molecules are used.<sup>39,40</sup> Solvation must play an important role, but it is difficult to probe.

It would, therefore, be interesting to see how these dynamics are influenced by changing the solvent, temperature, the composition of the monolayers or the chemical nature of one or two of the legs of the molecular hexapod. This will further develop our understanding of the dynamics of molecules in self-assembled monolayers, bring insight into solvation at solid–liquid interfaces, and lead to additional understanding in the multivalency concept.

## METHODS

**Scanning Tunneling Microscopy.** All experiments were performed at 20–22 °C. Scanning tunneling microscopy experiments were performed using a Topometrix Discoverer (using the constant-height mode) or PicoSPM (Agilent) (using the constant-current mode). Pt/Ir STM tips were prepared by mechanical cutting or electrochemical etching from Pt/Ir wire (80%/20%, diameter 0.2 mm) in 2 N KOH/6 N NaCN solution in water. Prior to imaging, the compounds under investigation were dissolved in 1-phenyloctane (Aldrich) at a concentration of approximately  $10^{-4}$  M, and a drop of this solution was applied on a freshly cleaved surface of highly oriented pyrolytic graphite (HOPG) (grade ZTB, Advanced Ceramics Inc., Cleveland, OH). Then, the STM tip was immersed into the solution and scanned: a bright (dark) contrast refers to a high (low) current/height. Only image 2A was recorded in the constant-current mode. The bias voltage was applied to the sample in such a way that, at negative bias voltage, electrons tunnel from the sample to the tip.

**Molecular Dynamics.** Molecular mechanics and molecular dynamics simulations have been carried out with the molecular modeling package TINKER 4.2, using MM3 force field. The surface is modeled by two frozen square slabs of graphite, and three-dimensional periodic boundary conditions have been applied to the system. In order to avoid self-interactions in the third dimension, a 50 Å thick vacuum slab has been placed above the surface. All of the simulations for an isolated hexapod on the surface have been conducted in the canonical NVT ensemble either at room temperature or at 650 K; the MD trajectories are several hundreds of picoseconds long, depending on the system, and the structural data for analysis are extracted from the last 150 ps of the MD run.

**Acknowledgment.** This work was supported by the Belgian Federal Science Policy Office via IAP-6/27, the Marie Curie Research Training Network CHEXTAN (MRTN-CT-2004-512161), the small-scale focused research project RESOLVE (NMP4-SL-2008-214340), the Belgian National Fund for Scientific Research (FRS-

FNRS), the Fund for Scientific Research-Flanders (FWO), and the Council for Chemical Sciences of The Netherlands Organization for Scientific Research (CW-NWO).

*Supporting Information Available:* Statistical analysis, molecular dynamics, STM movie of the dynamics. This material is available free of charge via the Internet at <http://pubs.acs.org>.

## REFERENCES AND NOTES

- Barth, J. V.; Costantini, G.; Kern, K. Engineering Atomic and Molecular Nanostructures at Surfaces. *Nature* **2005**, *437*, 671–679.
- De Feyter, S.; De Schryver, F. C. Self-Assembly at the Liquid/Solid Interface: STM Reveals. *J. Phys. Chem. B* **2005**, *109*, 4290–4302.
- Elemans, J. A. A. W.; De Feyter, S. Structure and Function Revealed with Submolecular Resolution at the Liquid–Solid Interface. *Soft Matter* **2009**, *5*, 721–735.
- Smith, R. K.; Weiss, P. S. Patterning Self-Assembled Monolayers. *Prog. Surf. Sci.* **2004**, *75*, 1–68.
- Binnig, G.; Rohrer, H.; Gerber, C.; Weibel, E. Surface Studies by Scanning Tunneling Microscopy. *Phys. Rev. Lett.* **1982**, *49*, 57–61.
- Yokoyama, T.; Yokoyama, S.; Okuno, Y.; Mashiko, S. Selective Assembly on a Surface of Supramolecular Aggregates with Controlled Size and Shape. *Nature* **2001**, *413*, 619–621.
- De Feyter, S.; De Schryver, F. C. Two-Dimensional Supramolecular Self-Assembly Probed by Scanning Tunneling Microscopy. *Chem. Soc. Rev.* **2003**, *32*, 139–150.
- Barth, J. V. Molecular Architectonic on Metal Surfaces. *Annu. Rev. Phys. Chem.* **2007**, *58*, 375–407.
- Rosei, F.; Schunack, M.; Naitoh, Y.; Jiang, P.; Gourdon, A.; Laegsgaard, E.; Stensgaard, I.; Joachim, C.; Besenbacher, F. Properties of Large Organic Molecules on Metal Surfaces. *Prog. Surf. Sci.* **2003**, *71*, 95–146.

10. Grill, L. Functionalized Molecules Studied by STM: Motion, Switching and Reactivity. *J. Phys.: Condens. Matter* **2008**, *20*, 053001-1–053001-19.
11. Berner, S.; Brunner, M.; Ramoino, L.; Suzuki, H.; Guntherodt, H.-J.; Jung, T. A. Time Evolution Analysis of a 2D Solid–Gas Equilibrium: A Model System for Molecular Adsorption and Diffusion. *Chem. Phys. Lett.* **2001**, *348*, 175–181.
12. Schunack, M.; Linderoth, T. R.; Rosei, F.; Laegsgaard, E.; Stensgaard, I.; Besenbacher, F. Long Jumps in the Surface Diffusion of Large Molecules. *Phys. Rev. Lett.* **2002**, *88*, 156102-1–156102-4.
13. Yanagi, H.; Mukai, H.; Ikuta, K.; Shibutani, T.; Kamikado, T.; Yokoyama, S.; Mashiko, S. Molecularly Resolved Dynamics for Two-Dimensional Nucleation of Supramolecular Assembly. *Nano Lett.* **2002**, *2*, 601–604.
14. Weckesser, J.; Barth, J. V.; Kern, K. Direct Observation of Surface Diffusion of Large Organic Molecules at Metal Surfaces: PVBA on Pd(110). *J. Chem. Phys.* **1999**, *43*, 5351–5354.
15. Otero, R.; Hummelink, F.; Sato, F.; Legoas, S. B.; Thostrup, P.; Laegsgaard, E.; Stensgaard, I.; Galvao, D. D.; Besenbacher, F. Lock-and-Key Effect in the Surface Diffusion of Large Organic Molecules Probed by STM. *Nat. Mater.* **2004**, *3*, 779–782.
16. Miwa, J. A.; Weigels, S.; Gersen, H.; Besenbacher, F.; Rosei, F.; Linderoth, T. R. Azobenzene on Cu(110): Adsorption Site-Dependent Diffusion. *J. Am. Chem. Soc.* **2006**, *128*, 3164–3165.
17. Schull, G.; Douillard, L.; Fiorini-Debuisschert, C.; Charra, F.; Mathevet, F.; Kreher, D.; Attias, A.-J. Selectivity of Single-Molecule Dynamics in 2D Molecular Sieves. *Adv. Mater.* **2006**, *18*, 2954–2957.
18. Schull, G.; Douillard, L.; Fiorini-Debuisschert, C.; Charra, F.; Mathevet, F.; Kreher, D.; Attias, A.-J. Single-Molecule Dynamics in a Self-Assembled 2D Molecular Sieve. *Nano Lett.* **2006**, *6*, 1360–1363.
19. Hou, S. M.; Sagara, T.; Xu, D. C.; Kelly, T. R.; Ganz, E. Investigation of Triptycene-Based Surface-Mounted Rotors. *Nanotechnology* **2003**, *14*, 566–570.
20. Wintjes, N.; Bonifazi, D.; Cheng, F. Y.; Kiebele, A.; Stohr, M.; Jung, T. A. A Supramolecular Multiposition Rotary Device. *Angew. Chem., Int. Ed.* **2007**, *46*, 4089–4092.
21. Wahl, M.; Stohr, M.; Spillmann, H.; Jung, T. A.; Gade, L. H. Rotation–Libration in a Hierarchic Supramolecular Rotor–Stator System: Arrhenius Activation and Retardation by Local Interaction. *Chem. Commun.* **2007**, *13*, 1349–1351.
22. Jung, T. A.; Schlittler, R. R.; Gimzewski, J. K. Conformational Identification of Individual Adsorbed Molecules with the STM. *Nature* **1997**, *386*, 696–698.
23. Scherer, L. J.; Merz, L.; Constable, E. C.; Housecroft, C. E.; Neuburger, M.; Hermann, B. A. Conformational Analysis of Self-Organized Monolayers with Scanning Tunneling Microscopy at Near-Atomic Resolution. *J. Am. Chem. Soc.* **2005**, *127*, 4033–4041.
24. Kim, K. B.; Plass, K. E.; Matzger, A. J. Conformational Pseudopolymorphism and Orientational Disorder in Two-Dimensional Alkyl Carbamate Crystals. *Langmuir* **2005**, *21*, 647–655.
25. Weigelt, S.; Busse, C.; Petersen, L.; Rauls, E.; Hammer, B.; Gothelf, K. V.; Besenbacher, F.; Linderoth, T. R. Chiral Switching by Spontaneous Conformational Change in Adsorbed Organic Molecules. *Nat. Mater.* **2006**, *5*, 112–117.
26. Busse, C.; Weigelt, S.; Petersen, L.; Laegsgaard, E.; Besenbacher, F.; Linderoth, T. R.; Thomsen, A. H.; Nielsen, M.; Gothelf, K. V. Chiral Ordering and Conformational Dynamics for a Class of Oligo-phenylene-ethynyls on Au(111). *J. Phys. Chem. B* **2007**, *111*, 5850–5860.
27. Lingenfelder, M.; Tomba, G.; Costantini, G.; Ciacchi, L. C.; De Vita, A.; Kern, K. Tracking the Chiral Recognition of Adsorbed Dipeptides at the Single-Molecule Level. *Angew. Chem., Int. Ed.* **2007**, *46*, 4492–4495.
28. Jung, T. A.; Schlittler, R. R.; Gimzewski, J. K.; Tang, H.; Joachim, C. Controlled Room-Temperature Positioning of Individual Molecules: Molecular Flexure and Motion. *Science* **1996**, *271*, 181–184.
29. Bohringer, M.; Morgenstern, K.; Schneider, W. D.; Berndt, R. Separation of a Racemic Mixture of Two-Dimensional Molecular Clusters by Scanning Tunneling Microscopy. *Angew. Chem., Int. Ed.* **1999**, *38*, 821–823.
30. Yanagi, H.; Ikuta, K.; Mukai, H.; Shibutani, T. STM-Induced Flip-Flop Switching of Adsorbed Subphthalocyanine Molecular Arrays. *Nano Lett.* **2002**, *2*, 951–955.
31. Elemans, J. A. A. W.; Lensen, M. C.; Gerritsen, J. W.; van Kempen, H.; Speller, S.; Nolte, R. J. M.; Rowan, A. E. Scanning Probe Studies of Porphyrin Assemblies and Their Supramolecular Manipulation at a Solid–Liquid Interface. *Adv. Mater.* **2003**, *15*, 2070–2073.
32. Moresco, F. Manipulation of Large Molecules by Low-Temperature STM: Model Systems for Molecular Electronics. *Phys. Rep.* **2004**, *399*, 175–225.
33. Griessl, S. J. H.; Lackinger, M.; Jamitzky, F.; Markert, T.; Hietschold, M.; Heckl, W. A. Incorporation and Manipulation of Coronene in an Organic Template Structure. *Langmuir* **2004**, *20*, 9403–9407.
34. Lorente, N.; Rurali, R.; Tang, H. Single-Molecule Manipulation and Chemistry with the STM. *J. Phys.: Condens. Matter* **2005**, *17*, S1049–S1074.
35. Stohr, M.; Wahl, M.; Spillmann, H.; Gade, L. H.; Jung, T. A. Lateral Manipulation for the Positioning of Molecular Guests within the Confinements of a Highly Stable Self-Assembled Organic Surface Network. *Small* **2007**, *3*, 1336–1340.
36. de Jonge, J. J.; Ratner, M. A.; de Leeuw, S. W. Local Field Controlled Switching in a One-Dimensional Dipolar Array. *J. Phys. Chem. C* **2007**, *111*, 3770–3777.
37. Meier, C.; Landfester, K.; Kunzel, D.; Markert, T.; Gross, A.; Ziener, U. Hierarchically Self-Assembled Host–Guest Network at the Solid–Liquid Interface for Single-Molecule Manipulation. *Angew. Chem., Int. Ed.* **2008**, *47*, 3821–3825.
38. Yang, Y. L.; Chan, Q. L.; Ma, X. J.; Deng, K.; Shen, Y. T.; Feng, X. Z.; Wang, C. Electrical Conformational Bistability of Dimesogen Molecules with a Molecular Chord Structure. *Angew. Chem., Int. Ed.* **2006**, *45*, 6889–6893.
39. Gesquiere, A.; Abdel-Mottaleb, M. M.; De Feyter, S.; De Schryver, F. C.; Sieffert, M.; Mullen, K.; Calderone, A.; Lazzaroni, R.; Bredas, J. L. Dynamics in Physisorbed Monolayers of 5-Alkoxy-isophthalic Acid Derivatives at the Liquid/Solid Interface Investigated by Scanning Tunneling Microscopy. *Chem.—Eur. J.* **2000**, *6*, 3739–3746.
40. Stevens, F.; Beebe, T. P. Dynamical Exchange Behavior in Organic Monolayers Studied by STM Analysis of Labeled Mixtures. *Langmuir* **1999**, *15*, 6884–6889.
41. Stabel, A.; Heinz, R.; De Schryver, F. C.; Rabe, J. P. Ostwald Ripening of Two-Dimensional Crystals at the Solid–Liquid Interface. *J. Phys. Chem.* **1995**, *99*, 505–507.
42. Samori, P.; Mullen, K.; Rabe, J. P. Molecular-Scale Tracking of the Self-Healing of Polycrystalline Monolayers at the Solid–Liquid Interface. *Adv. Mater.* **2004**, *16*, 1761–1765.
43. Florio, G. M.; Klare, J. E.; Pasamba, M. O.; Werblowsky, T. L.; Hyers, M.; Berne, B. J.; Hybertsen, M. S.; Nuckolls, C.; Flynn, G. W. Frustrated Ostwald Ripening in Self-Assembled Monolayers of Cruciform  $\pi$ -Systems. *Langmuir* **2006**, *22*, 10003–10008.
44. Hermann, B. A.; Scherer, L. J.; Housecroft, C. E.; Constable, E. C. Self-Organized Monolayers: A Route to Conformational Switching and Read-Out of Functional Supramolecular Assemblies by Scanning Probe Methods. *Adv. Funct. Mater.* **2006**, *16*, 221–235.
45. Rohde, D.; Yan, C. J.; Yan, H. J.; Wan, L. J. From a Lamellar to Hexagonal Self-Assembly of Bis(4,4'-(*m,m'*-di(dodecyloxy)phenyl)-2,2'-difluoro-1,3,2-dioxaborin) Molecules: A trans-to-cis-Isomerization-Induced Structural Transition Studied with STM. *Angew. Chem., Int. Ed.* **2006**, *45*, 3996–4000.



46. Badjic, J. D.; Nelson, A.; Cantrill, S. J.; Turnbull, W. B.; Stoddart, J. F. Multivalency and Cooperativity in Supramolecular Chemistry. *Acc. Chem. Res.* **2005**, *38*, 723–732.
47. Mulder, A.; Huskens, J.; Reinhoudt, D. N. Multivalency in Supramolecular Chemistry and Nanofabrication. *Org. Biomol. Chem.* **2004**, *2*, 3409–3424.
48. Tomovic, Z.; van Dongen, J.; George, S. J.; Xu, H.; Pisula, W.; Leclere, P.; De Feyter, S.; Meijer, E. W.; Schenning, A. P. H. J. Star-Shaped Oligo(*p*-phenylenevinylene) Substituted Hexaarylbenzene: Purity, Stability, and Chiral Self-Assembly. *J. Am. Chem. Soc.* **2007**, *129*, 16190–16196.
49. *TINKER*, Software Tools for Molecular Design (<http://dasher/wustl.edu/tinker>).
50. Ma, B. Y.; Lii, J. H.; Allinger, N. L. Molecular Polarizabilities and Induced Dipole Moments in Molecular Mechanics. *J. Comput. Chem.* **2000**, *21*, 813–825.
51. Broeren, M. A. C.; van Dongen, J. L. J.; Pittelkow, M.; Christensen, J. B.; van Genderen, M. H. P.; Meijer, E. W. Multivalency in the Gas Phase: The Study of Dendritic Aggregates by Mass Spectrometry. *Angew. Chem., Int. Ed.* **2004**, *43*, 3557–3562.
52. Stabel, A.; Heinz, R.; Rabe, J. P.; Wegner, G.; De Schryver, F. C.; Corens, D.; Dehaen, W.; Siiling, C. STM Investigation of 2D Crystals of Anthrone Derivatives on Graphite: Analysis of Molecular Structure and Dynamics. *J. Phys. Chem.* **1995**, *99*, 8690–8697.